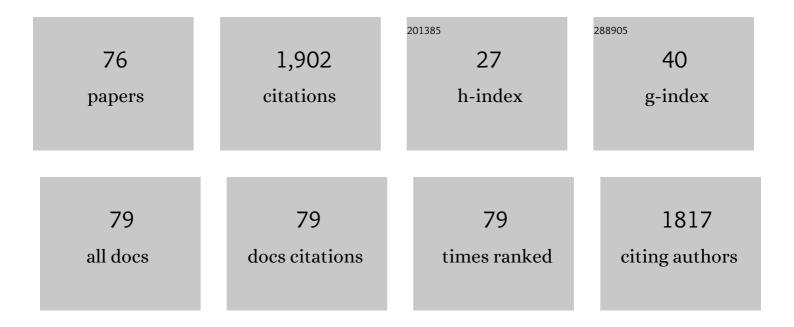
Michael W Jenkins

List of Publications by Year in descending order

Source: https://exaly.com/author-pdf/6658350/publications.pdf Version: 2024-02-01



#	Article	IF	CITATIONS
1	Slide Over. American Journal of Pathology, 2022, 192, 180-194.	1.9	10
2	Glutathione Protects the Developing Heart from Defects and Global DNA Hypomethylation Induced by Prenatal Alcohol Exposure. Alcoholism: Clinical and Experimental Research, 2021, 45, 69-78.	1.4	9
3	Nuclei Detection for 3D Microscopy With a Fully Convolutional Regression Network. IEEE Access, 2021, 9, 60396-60408.	2.6	8
4	Isotonic ion replacement can lower the threshold for selective infrared neural inhibition. Neurophotonics, 2021, 8, 015005.	1.7	4
5	Pocket MUSE: an affordable, versatile and high-performance fluorescence microscope using a smartphone. Communications Biology, 2021, 4, 334.	2.0	33
6	3D imaging of the vagus nerve fascicular anatomy with cryo-imaging and UV excitation. , 2021, 11649, .		3
7	Glutathione ethyl ester reverses the deleterious effects of fentanyl on ventilation and arterial blood-gas chemistry while prolonging fentanyl-induced analgesia. Scientific Reports, 2021, 11, 6985.	1.6	18
8	Optimizing thermal block length during infrared neural inhibition to minimize temperature thresholds. Journal of Neural Engineering, 2021, 18, 056016.	1.8	7
9	Folic acid prevents functional and structural heart defects induced by prenatal ethanol exposure. American Journal of Physiology - Heart and Circulatory Physiology, 2021, 320, H1313-H1320.	1.5	4
10	Systemic Administration of Tempol Attenuates the Cardiorespiratory Depressant Effects of Fentanyl. Frontiers in Pharmacology, 2021, 12, 690407.	1.6	14
11	Prenatal ethanol exposure impairs the conduction delay at the atrioventricular junction in the looping heart. American Journal of Physiology - Heart and Circulatory Physiology, 2021, 321, H294-H305.	1.5	3
12	Characterization of endothelium-dependent and -independent processes in occipital artery of the rat: relevance to control of blood flow to nodose sensory cells. Journal of Applied Physiology, 2021, 131, 1067-1079.	1.2	2
13	CompassLSM: axially swept light-sheet microscopy made simple. Biomedical Optics Express, 2021, 12, 6571.	1.5	5
14	Polarization-sensitive optical coherence tomography monitoring of percutaneous radiofrequency ablation in left atrium of living swine. Scientific Reports, 2021, 11, 24330.	1.6	8
15	Identifying the Role of Block Length in Neural Heat Block to Reduce Temperatures During Infrared Neural Inhibition. Lasers in Surgery and Medicine, 2020, 52, 259-275.	1.1	14
16	Three-dimensional alignment of microvasculature and cardiomyocytes in the developing ventricle. Scientific Reports, 2020, 10, 14955.	1.6	5
17	NADPH diaphorase detects S-nitrosylated proteins in aldehyde-treated biological tissues. Scientific Reports, 2020, 10, 21088.	1.6	15
18	Genetically Encoded Calcium Indicators for In Situ Functional Studies of Corneal Nerves. , 2020, 61, 10.		1

Genetically Encoded Calcium Indicators for In Situ Functional Studies of Corneal Nerves. , 2020, 61, 10. 18

MICHAEL W JENKINS

#	Article	IF	CITATIONS
19	Semi-automated shear stress measurements in developing embryonic hearts. Biomedical Optics Express, 2020, 11, 5297.	1.5	1
20	Intracardiac radiofrequency ablation in living swine guided by polarization-sensitive optical coherence tomography. Journal of Biomedical Optics, 2020, 25, 1.	1.4	4
21	Noninvasive Assessment of Corneal Crosslinking With Phase-Decorrelation Optical Coherence Tomography. , 2019, 60, 41.		26
22	SLIME: robust, high-speed 3D microvascular mapping. Scientific Reports, 2019, 9, 893.	1.6	5
23	Thermal block of action potentials is primarily due to voltage-dependent potassium currents: a modeling study. Journal of Neural Engineering, 2019, 16, 036020.	1.8	36
24	A Review of Structural and Biomechanical Changes in the Cornea in Aging, Disease, and Photochemical Crosslinking. Frontiers in Bioengineering and Biotechnology, 2019, 7, 66.	2.0	102
25	Adamts10 inactivation in mice leads to persistence of ocular microfibrils subsequent to reduced fibrillin-2 cleavage. Matrix Biology, 2019, 77, 117-128.	1.5	40
26	Voltage-gated potassium channels are critical for infrared inhibition of action potentials: an experimental study. Neurophotonics, 2019, 6, 1.	1.7	26
27	Localization and induced release of potentially therapeutic components of the rat submandibular salivary gland. FASEB Journal, 2019, 33, 446.3.	0.2	Ο
28	Removing vessel constriction on the embryonic heart results in changes in valve gene expression, morphology, and hemodynamics. Developmental Dynamics, 2018, 247, 531-541.	0.8	10
29	Complex regression Doppler optical coherence tomography. Journal of Biomedical Optics, 2018, 23, 1.	1.4	3
30	Integrated RFA/PSOCT catheter for real-time guidance of cardiac radio-frequency ablation. Biomedical Optics Express, 2018, 9, 6400.	1.5	28
31	Increased regurgitant flow causes endocardial cushion defects in an avian embryonic model of congenital heart disease. Congenital Heart Disease, 2017, 12, 322-331.	0.0	28
32	Supplementation with the Methyl Donor Betaine Prevents Congenital Defects Induced by Prenatal Alcohol Exposure. Alcoholism: Clinical and Experimental Research, 2017, 41, 1917-1927.	1.4	28
33	Selective inhibition of small-diameter axons using infrared light. Scientific Reports, 2017, 7, 3275.	1.6	47
34	Molecular Consequences of Cardiac Valve Development as a Result of Altered Hemodynamics. Microscopy and Microanalysis, 2017, 23, 1330-1331.	0.2	0
35	Embryonic aortic arch hemodynamics are a functional biomarker for ethanol-induced congenital heart defects [Invited]. Biomedical Optics Express, 2017, 8, 1823.	1.5	14
36	An infrared optical pacing system for screening cardiac electrophysiology in human cardiomyocytes. PLoS ONE, 2017, 12, e0183761.	1.1	27

MICHAEL W JENKINS

#	Article	IF	CITATIONS
37	Complex decorrelation averaging in optical coherence tomography: a way to reduce the effect of multiple scattering and improve image contrast in a dynamic scattering medium. Optics Letters, 2017, 42, 2738.	1.7	11
38	Probing the Electrophysiology of the Developing Heart. Journal of Cardiovascular Development and Disease, 2016, 3, 10.	0.8	6
39	Volumetric optical mapping in early embryonic hearts using light-sheet microscopy. Biomedical Optics Express, 2016, 7, 5120.	1.5	10
40	CUGâ€BP, Elavâ€like family member 1 (CELF1) is required for normal myofibrillogenesis, morphogenesis, and contractile function in the embryonic heart. Developmental Dynamics, 2016, 245, 854-873.	0.8	4
41	Cardiac neural crest ablation results in early endocardial cushion and hemodynamic flow abnormalities. American Journal of Physiology - Heart and Circulatory Physiology, 2016, 311, H1150-H1159.	1.5	21
42	Infrared inhibition of embryonic hearts. Journal of Biomedical Optics, 2016, 21, 1.	1.4	30
43	Impaired ADAMTS9 secretion: A potential mechanism for eye defects in Peters Plus Syndrome. Scientific Reports, 2016, 6, 33974.	1.6	28
44	Modeling the effects of elevated temperatures on action potential propagation in unmyelinated axons. Proceedings of SPIE, 2016, , .	0.8	3
45	Using optical coherence tomography to rapidly phenotype and quantify congenital heart defects associated with prenatal alcohol exposure. Developmental Dynamics, 2015, 244, 607-618.	0.8	27
46	Muscleblind-like 1 is required for normal heart valve development in vivo. BMC Developmental Biology, 2015, 15, 36.	2.1	7
47	Optical coherence tomography imaging of the patent ductus arteriosus: First known uses in congenital heart disease. Catheterization and Cardiovascular Interventions, 2015, 85, 278-281.	0.7	2
48	3-D Stent Detection in Intravascular OCT Using a Bayesian Network and Graph Search. IEEE Transactions on Medical Imaging, 2015, 34, 1549-1561.	5.4	50
49	Miniature forward-viewing common-path OCT probe for imaging the renal pelvis. Biomedical Optics Express, 2015, 6, 1164.	1.5	16
50	Mapping conduction velocity of early embryonic hearts with a robust fitting algorithm. Biomedical Optics Express, 2015, 6, 2138.	1.5	11
51	Three-dimensional correction of conduction velocity in the embryonic heart using integrated optical mapping and optical coherence tomography. Journal of Biomedical Optics, 2014, 19, 076004.	1.4	14
52	Capturing structure and function in an embryonic heart with biophotonic tools. Frontiers in Physiology, 2014, 5, 351.	1.3	23
53	Alternating current and infrared produce an onset-free reversible nerve block. Neurophotonics, 2014, 1, 011010.	1.7	30
54	Orientation-independent rapid pulsatile flow measurement using dual-angle Doppler OCT. Biomedical Optics Express, 2014, 5, 499.	1.5	16

MICHAEL W JENKINS

#	Article	IF	CITATIONS
55	Optical stimulation enables paced electrophysiological studies in embryonic hearts. Biomedical Optics Express, 2014, 5, 1000.	1.5	19
56	Connecting teratogenâ€induced congenital heart defects to neural crest cells and their effect on cardiac function. Birth Defects Research Part C: Embryo Today Reviews, 2014, 102, 227-250.	3.6	17
57	Ethanol exposure alters early cardiac function in the looping heart: a mechanism for congenital heart defects?. American Journal of Physiology - Heart and Circulatory Physiology, 2014, 306, H414-H421.	1.5	59
58	Fiber-optic catheter-based polarization-sensitive OCT for radio-frequency ablation monitoring. Optics Letters, 2014, 39, 5066.	1.7	51
59	Optical pacing of the adult rabbit heart. Biomedical Optics Express, 2013, 4, 1626.	1.5	54
60	Transient and selective suppression of neural activity with infrared light. Scientific Reports, 2013, 3, 2600.	1.6	114
61	Spatial and temporal variability in response to hybrid electro-optical stimulation. Journal of Neural Engineering, 2012, 9, 036003.	1.8	64
62	4D shear stress maps of the developing heart using Doppler optical coherence tomography. Biomedical Optics Express, 2012, 3, 3022.	1.5	50
63	Longitudinal Imaging of Heart Development With Optical Coherence Tomography. IEEE Journal of Selected Topics in Quantum Electronics, 2012, 18, 1166-1175.	1.9	43
64	Optical coherence tomography captures rapid hemodynamic responses to acute hypoxia in the cardiovascular system of early embryos. Developmental Dynamics, 2012, 241, 534-544.	0.8	23
65	Motion artifacts associated with in vivo endoscopic OCT images of the esophagus. Optics Express, 2011, 19, 20722.	1.7	46
66	Optical Coherence Tomography Imaging of Early Quail Embryos. Cold Spring Harbor Protocols, 2011, 2011, pdb.prot5564.	0.2	5
67	Blood flow dynamics of one cardiac cycle and relationship to mechanotransduction and trabeculation during heart looping. American Journal of Physiology - Heart and Circulatory Physiology, 2011, 300, H879-H891.	1.5	56
68	High-Speed Optical Coherence Tomography Imaging of the Beating Avian Embryonic Heart. Cold Spring Harbor Protocols, 2011, 2011, pdb.top98-pdb.top98.	0.2	9
69	Measuring hemodynamics in the developing heart tube with four-dimensional gated Doppler optical coherence tomography. Journal of Biomedical Optics, 2010, 15, 066022.	1.4	57
70	Endoscopically guided spectral-domain OCT with double-balloon catheters. Optics Express, 2010, 18, 17364.	1.7	32
71	High temporal resolution OCT using image-based retrospective gating. Optics Express, 2009, 17, 10786.	1.7	86
72	A combined multiple-SLED broadband light source at 1300nm for high resolution optical coherence tomography. Optics Communications, 2008, 281, 1896-1900.	1.0	12

#	Article	IF	CITATIONS
73	Denoising and 4D visualization of OCT images. Optics Express, 2008, 16, 12313.	1.7	76
74	In vivo gated 4D imaging of the embryonic heart using optical coherence tomography. Journal of Biomedical Optics, 2007, 12, 030505.	1.4	81
75	Phenotyping transgenic embryonic murine hearts using optical coherence tomography. Applied Optics, 2007, 46, 1776.	2.1	33
76	Optical Coherence Tomography Imaging of the Purkinje Network. Journal of Cardiovascular Electrophysiology, 2005, 16, 559-560.	0.8	15